AIAA 2001-2564

The Lag Model, a Turbulence Model for Wall Bounded Flows Including Separation

M. E. Olsen
T. J. Coakley
NASA Ames Research Center
Moffett Field, CA 94035

15th AIAA Fluid Dynamics Conference
June 11 - June 14, 2001 / Anaheim, CA

The Lag Model, a Turbulence Model for Wall Bounded Flows Including Separation

M. E. Olsen *

T. J. Coakley †

NASA Ames Research Center

Moffett Field, CA 94035

A new class of turbulence model is described for wall bounded, high Reynolds number flows. A specific turbulence model is demonstrated, with results for favorable and adverse pressure gradient flowfields. Separation predictions are as good or better than either Spalart Almaras or SST models, do not require specification of wall distance, and have similar or reduced computational effort compared with these models.

Introduction

One difficulty with current one and two-equation turbulence models is the inability to account directly for non-equilibrium effects such as those encountered in large pressure gradients involving separation and shockwaves. Current turbulence models such as Spalart's one-equation model,[5] the classic $k - \epsilon$ and Wilcox's $k - \omega$[1] two-equation models have been designed and tuned to accurately predict equilibrium flows such as zero-pressure gradient boundary- layers and free shear layers. Application in more complex flows can be problematical at best. Although there have been many attempts to modify or correct basic one- and two-equation models, most of these attempts have been only marginally successful in predicting complex flows.

More complex models such as Reynolds stress models have been investigated extensively, primarily for relatively simple flows but also for complex flows. In most cases these models give somewhat better predictions than the simpler one and two equation models, but for complex flows they do not perform much better than the simpler models. One theoretical advantage of Reynolds stress models is that they directly account for non-equilibrium effects in the sense that the Reynolds stresses do not respond instantaneously to changes to the strain rate but more realistically lag them in time and/or space. Unfortunately, The Reynolds stress models are usually considerably more complicated and numerically stiff than the one- and two- equation models, and this has prevented their wide application for complex flows.

In this paper we introduce a new three equation model designed to account for non-equilibrium effects without invoking the full formalism of the Reynolds stress models. The basic idea is to take a baseline two-equation model and to couple it with a third (lag) equation to model the non-equilibrium effects for the eddy viscosity. The third equation is designed to predict the equilibrium eddy viscosity in equilibrium flows.

We show results obtained with a lag model based on the Wilcox k-ω model. Applications to four flows are given including an essentially incompressible flat plate flows, an essentially incompressible adverse pressure gradient flow with separation,[2] a transonic bump flow[3] with a shock wave and separation, a three dimensional transonic wing flow.[4] Results using the new model are compared with results obtained with Spalart's model[5] and Menter's k-ω SST model.[6] Results obtained with the new model show encouraging improvements over results obtained with the other models.

The Lag Model

The differential equations defining the lag model are

$$\rho \frac{Dk}{Dt} = \mathcal{P}_k - \epsilon_k + \vec{\nabla}(\mu + \sigma_k \rho \nu_t \vec{\nabla} k) \quad (1)$$

$$\rho \frac{D\omega}{Dt} = \mathcal{P}_\omega - \epsilon_\omega + \vec{\nabla}(\mu + \sigma_\omega \rho \nu_t \vec{\nabla} \omega) \quad (2)$$

$$\rho \frac{D\nu_t}{Dt} = a(R_T) \rho \omega (\nu_{t_E} - \nu_t) \quad (3)$$

where:

$$\nu_{t_E} = k/\omega \qquad R_t = \rho k/\mu \omega$$

$$\mathcal{P}_k = \rho \nu_t S^2 \qquad \mathcal{P}_\omega = \alpha \rho S^2$$

$$\epsilon_k = \beta^* \rho k \omega \qquad \epsilon_\omega = \beta \rho \omega^2$$

$$S = \sqrt{2 s_{ij} s_{ij}}$$

$$s_{ij} = \frac{1}{2}(\frac{\partial u_i}{\partial x_j} + \frac{\partial u_j}{\partial x_i})$$

* Research Scientist, NASA Ames Research Center, Associate Fellow AIAA

† Research Scientist, NASA Ames Research Center, Associate Fellow AIAA

$$\alpha(R_T) = \alpha_0 \left[\frac{(R_T + R_{T_0})}{(R_T + R_{T\infty})} \right] \qquad (4)$$

with parameters

		α	$= 5/9$
α_0	$= 0.35$	β	$= 0.075$
R_{T_0}	$= 1$	β^*	$= 0.09$
$R_{T\infty}$	$= .01$	σ_k	$= 0.5$
		σ_ϵ	$= 0.5$

The model equations are composed of an underlying model, $(k - \omega)$ with the lag equation augmenting the system. The $k - \omega$ model, given by the first two equations is unchanged from the standard model, except that ν_t is now given by a field PDE, Eq.(3), instead of k/ω.

The boundary conditions are those of a convected scalar: specified on inflow boundaries and extrapolated on outflow boundaries. At inflow boundaries, k, ω and ν_t are set to constants (hereafter referred to as k_∞, ω_∞, and $\nu_{t\infty} = k_\infty/\omega_\infty$). In this paper, k_∞/U_∞^2 was chosen to be 0.0001, corresponding to a turbulent intensity of 0.8%. The value of k external to the wall bounded flows is, of course, substantially lower than this, since k decays in the absence of mean strains. ω_∞ is chosen to yield a low value of ν_{t_ℓ} (here chosen as one tenth the molecular ν), and ν_t is set to ν_{t_ℓ}. The model's predictions are insensitive to the values chosen for these constants as is shown in the results. At the solid walls a "no lag" boundary condition is enforced: the eddy viscosity is set to its equilibrium value: zero for hydraulicly smooth walls, finite for rough walls. The cases discussed in this paper all use the smooth wall conditions.[7] Rough wall boundary conditions are also possible in the manner of the $k - \omega$ model,[2] but are not discussed in this paper.

The turbulent eddy viscosity is governed by Eq.(3). This equation simply says that the eddy viscosity goes to its equilibrium value (ν_{t_ℓ}) along a streamline like a first order dynamical system with a time constant given by $1/(\alpha\omega)$. The stability of the turbulence model as a dynamical system is ensured by the form of this source term, given a stable underlying model. There is no diffusion term in this equation, and evolution of the eddy viscosity is dependent only on its upstream history and the underlying equilibrium eddy viscosity at that point.

The α term of Eq.3 of the source for the ν_T Eq.(4) governs the amount of lag present in the model. This term is made up of three factors. The leading constant, α_0, controls the amount of lag in the model. The higher the value of α_0, the less lag(shorter time constant) in the system, and the closer will follow the underlying turbulence model. The second factor in Eq.4 goes monotonically from 100 to one as R_T goes from 0 to infinity(Fig. 1). This in effect stiffens the
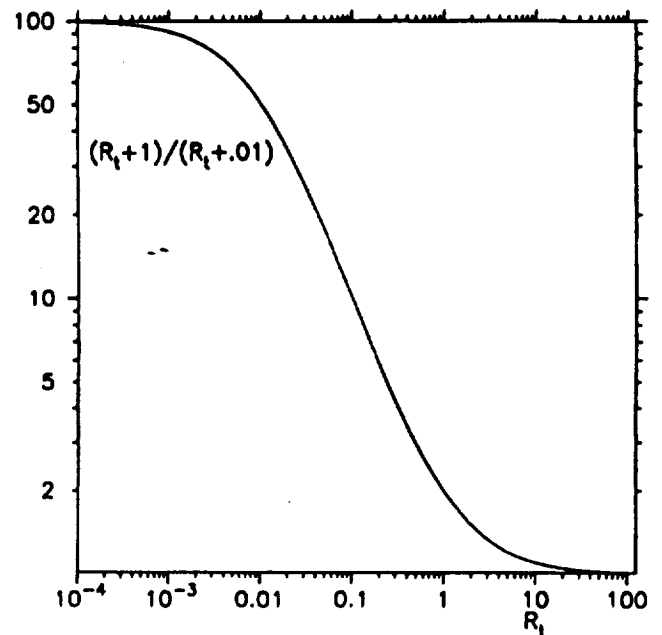

Fig. 1 Lag Source R_T Factor

model at low values of R_T so that it will have less lag, and will act more like the unmodified model in these conditions. In effect, this term "turns on" the lag only in turbulent regions ($R_T \gg 1$).

The model requires the storage of one additional field variable over the SST model, but does not require the wall distance information used in both the SST and SA models, thus freeing up the storage required for that variable. As the model is computationally simple, not requiring the $\vec{\nabla}\nu_t \cdot \vec{\nabla}\nu_t$ or $\vec{\nabla}k \cdot \vec{\nabla}\omega$ terms present in the other models, it actually requires less CPU time per iteration than either SST or SA models, and similar or fewer iterations for convergence.

Numerical Method

The solutions obtained in this paper were done with a modified version of the OVERFLOW[8,9] code. For the mean flow equations, the existing 3rd order upwind scheme or the central/matrix dissipation[10] method was used. The full Navier Stokes equations were solved, as opposed to utilizing the thin layer approximation. Converged solutions were indistinguishable in terms of skin friction and velocity profiles. Matrix dissipation was used with 2nd and 4th order smoothing coefficients of 2 and 0.1, respectively. The eigenvalue limiters were set to zero, and Roe averaging was used to form the matrix. Multigrid was employed, both as grid sequencing for startup, and during the relaxation process. 3 levels of multigrid were used for all solutions presented in this paper.

The turbulence model equations were spatially discretized using a 2nd order upwind method with a min-mod limiter. This is a departure from the 2 equation models implemented in OVERFLOW, which use 1st order upwind. 1st order upwind was the initial

2
American Institute of Aeronautics and Astronautics

presented in this paper.

The turbulence model equations was spatially discretized using a 2nd order upwind method with a min-mod limiter. This is a departure from the 2 equation models implemented in OVERFLOW, which use 1st order upwind. 1st order upwind was the initial implementation, but this proved too dissipative, and led to excessive grid density requirements for grid independent solutions.

The reason for this can be seen in the 3rd equation, which implements the history effects (lag) of the model. Using a 1st order upwind on this equation is analogous to using a 1st order time integrator to integrate an ODE, with grid spacing analogous to the ODE time step size. When the 1st order upwinding was replaced with a 2nd upwinding, the gridding requirements dropped back to what would normally be required for grid independent solutions with other turbulence models. The additional work required to solve the third equation is offset by the relative simplicity of the underlying model. Convergence is rapid and robust, as implemented in OVERFLOW.

Results

Dissipation of Isotropic Turbulence

Isotropic turbulence has no mean strain, so that the decay of k and ω follow those of the underlying model, here the Wilcox $k - \omega$ model. The ν_t equation uncouples from the other two equations, and the equation governing the evolution of the eddy viscosity becomes:

$$\frac{\partial \nu_t}{\partial t} = a_0(k - \omega \nu_t)$$

This decoupling is aesthetically beautiful, from the viewpoint of ν_t as a ratio of turbulent stess to mean strain. When the mean strain vanishes the turbulent stresses are not effected by the value of the eddy viscosity. Similarly, the lag equation does not affect the decay of turbulent kinetic energy built into the underlying model under conditions of zero mean strain.

Equilibrium Channel Flows

For fully developed channel shear flows, such as Couette, or fully developed pipe flows, the model again decouples and reproduces the results of the underlying model. The differential equation becomes:

$$u\frac{\partial \nu_t}{\partial x} = a_0(k - \omega \nu_t)$$

and as $\frac{\partial \nu_t}{\partial x} = 0$ for fully developed Couette or channel flows, this simply enforces $\nu_t = k/\omega$. In the same manner as in the decay of isotropic turbulence, if the underlying model does a good job under these conditions (which $k - \omega$ does) then the Lag model will also.

Subsonic Flat Plate

The fine grid for this case is 101(streamwise)×101(wall normal). Nearly identical results were obtained on a 51×51 grid. The wall normal grid stretching for these cases was 1.1 and 1.2 respectively, with initial y^+ spacings of 0.1 and 0.2. The initial 4 wall normal points were equispaced.
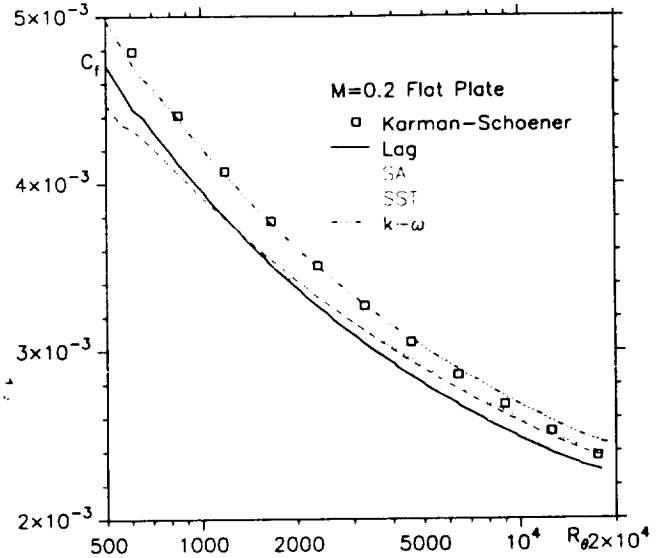

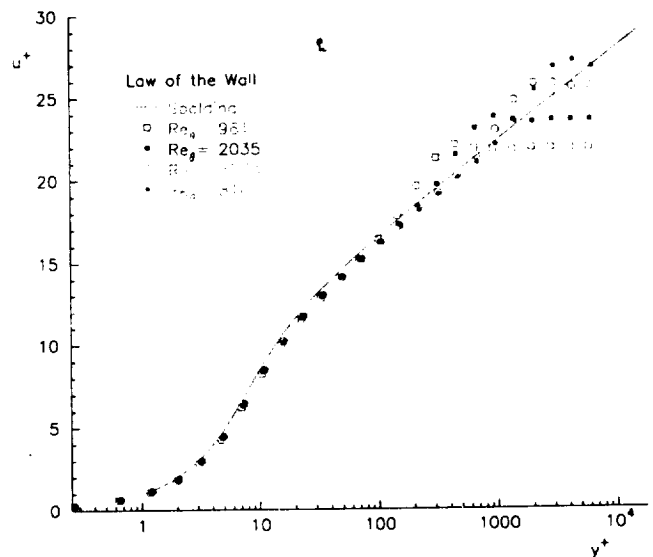**Fig. 2 Subsonic Flat Plate Skin Friction**

Fig. 3 Law of the Wall Velocity Profiles

For flat plates, the model roughly reproduces the original model performance, since the flow is slowly varying in the streamwise direction, and the model forces ν_t to its equilibrium values. Comparison for low speed flows (actually $M_\infty = 0.2$, Fig.) shows a good comparison with Karman-Schoener correlation. This was expected from the underlying $k - \omega$ model's predictions for smooth flat plates. The law of the wall is also well reproduced (Fig. 3).
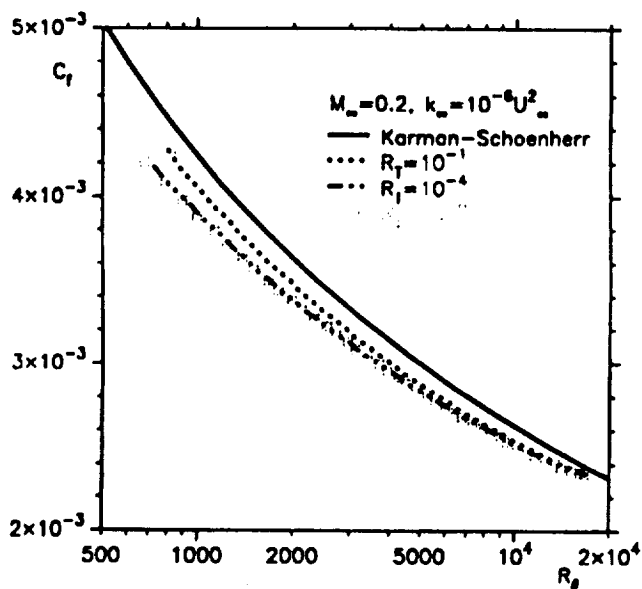
3
American Institute of Aeronautics and Astronautics

Fig. 4 ω_∞ Dependence

wall distance information, and are under consideration for use as future baseline models. The y^+ requirements were also investigated, and similar behaviour to the underlying $k - \omega$ model were found.[7] Improvements and extensions of the which include roughness are available for the $k - \omega$ model,[13] and are also under consideration for future model improvement.

Driver CS0 Separated Case

This is a low speed separated case.[3] The axisymmetric geometry (Fig. 5) is defined by an external streamline determined from experimental data, and wall pressures are available in addition to velocity profiles and skin friction.

Fig. 5 Driver CS0 Flowfield

Upstream boundary conditions were constant total pressure and temperature, with static pressure allowed to vary and velocity direction aligned with the cylinder axis. The outer streamline was treated as an inviscid wall. The viscous wall(the surface of a cylinder) is a no-slip, adiabatic wall. The downstream static pressure was adjusted to match the experimental static pressure (Fig. 6) upstream of the interaction region(x $\approx$ −.438m). Upstream length of the cylindrical body was adjusted so that the computed the boundary layer thickness at x = −0.438m matched the experiment. This "entry length" was the same for all three models.

The standard OVERFLOW low Mach number preconditioning was employed. The grid used in these calculations was 200(axial) by 160(radial), an extremely fine grid. The calculations were repeated with a
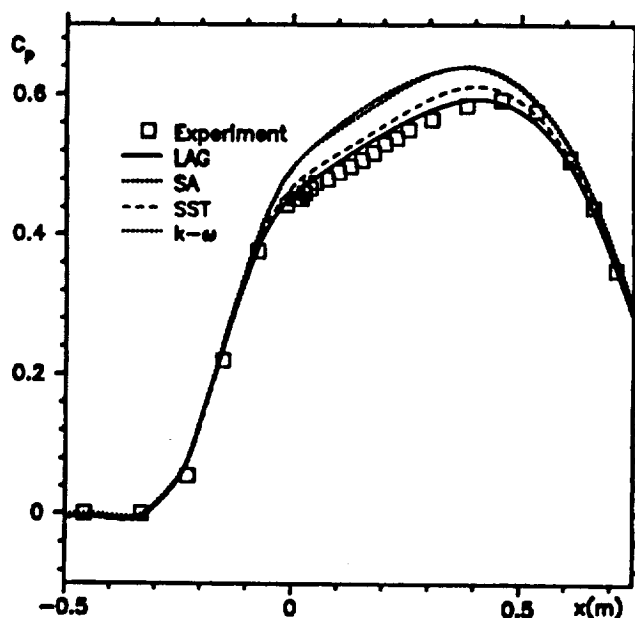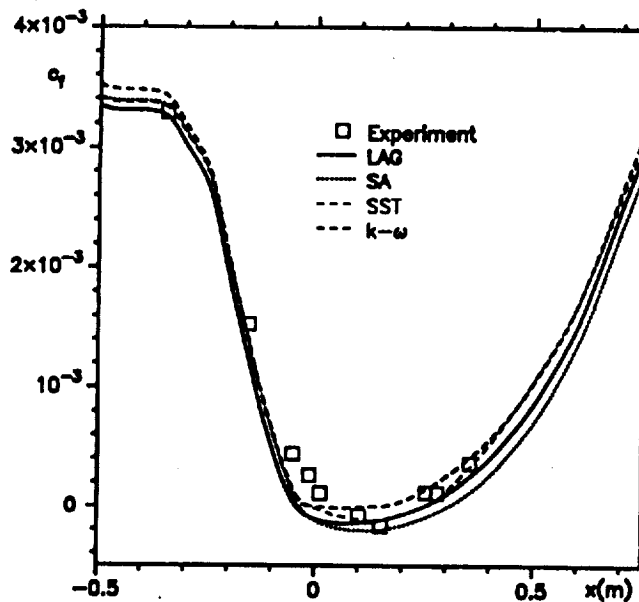

Fig. 6 Driver CS0 Surface Pressures

Fig. 7 Driver CS0 Skin Friction

100 × 80 grid and demonstrated grid independence in the same manner as Bardina et. al.[7] Surface pressures, skin friction and velocity profiles agreed with the fine grid results. This case was one which demonstrated the need for handling the turbulence model convection operator with 2nd order upwind (minmod limiter), as the solutions on the two grids are effectively identical when the 2nd order operator is employed, but show slight differences when computed with a first order upwind operator for the turbulence model.

The pressure variation predicted by the Lag model is closer to the experimental data than either the Spalart-Almaras or SST models, although both give reasonable agreement. This improvement in pressure variation prediction could be important for internal
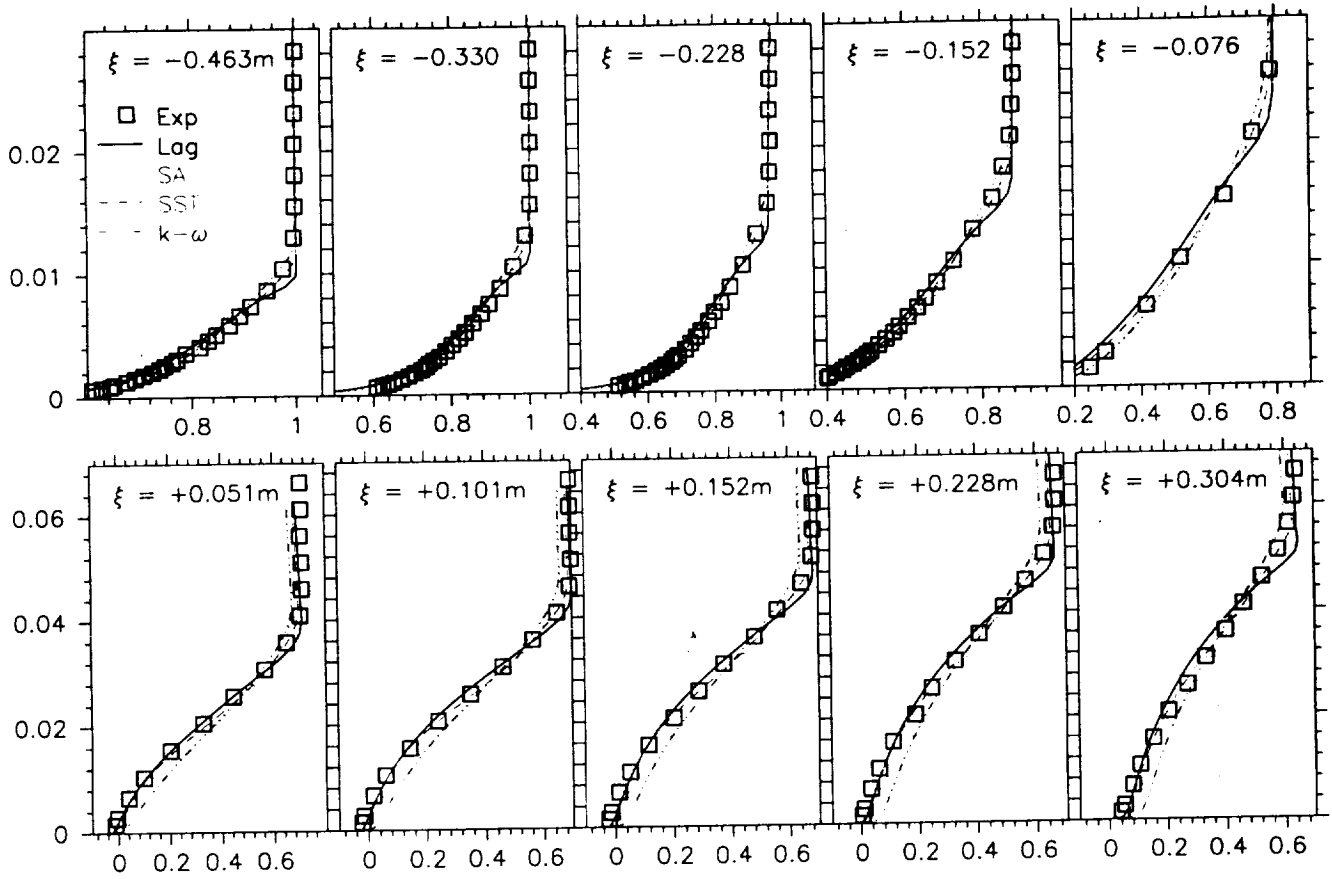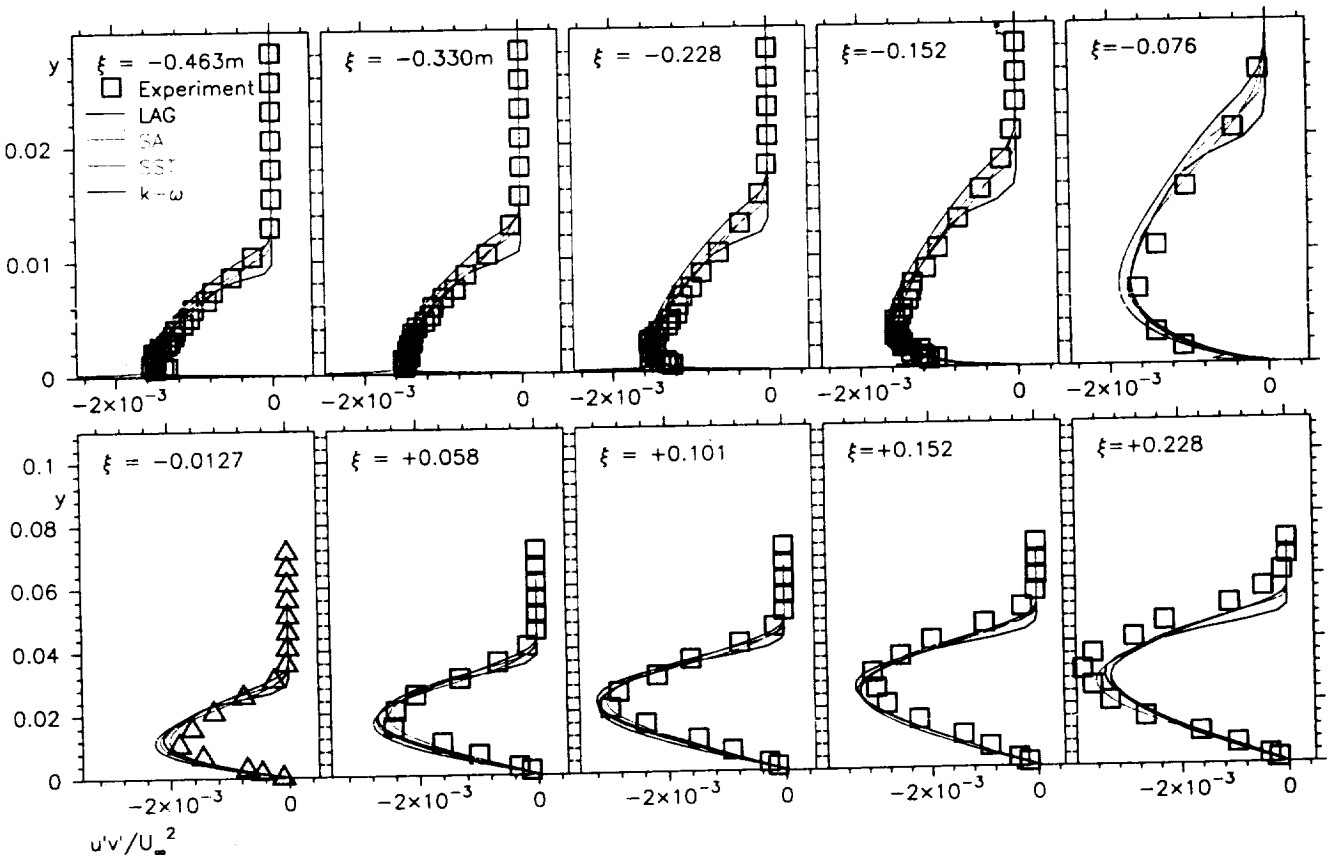
Fig. 8 Driver CS0 Velocity Profiles

Fig. 9 Driver CS0 Stress Profiles

low speed flows with small separations. The model's ability to more accurately predict the pressure variations will be repeated in later test cases.

The skin friction prediction of all four models is shown in Fig. 7. All four predict the skin friction reasonably well, with the SA model predicting a reattachment point slightly downstream of the experimental data and the $k - \omega$ model failing to predict separation. All models predict c_f too low just upstream of separation, from $x = -.1$ to $x = 0$.

The velocity profiles (Fig. 8) also show good agreement. The differences between the underlying $k - \omega$ model and the lag model are relatively small upstream of separation, but the lag model predicts the separated profiles more accurately in the separated region $(x > 0)$.

The shear stress profiles are similarly well predicted (Fig. 9), for both the evolution of the maximum shear stress and its location. The lag of the model is evident most clearly in this figure. Upstream of the separation, the shear stress predicted by the lag model is true to it's name, and lags the underlying $k - \omega$ model especially evidently at the $\xi = -0.076$ station. By the $\xi = 0.101$ station, all of the models are predicting roughly the same shear stress, even though the velocity profile predictions (Fig. 8) show the greatest scatter at this location. One of the model's slight imperfections can be seen in Fig.8 and Fig.9, as the outer edge of the boundary layer has a kink not seen in the other models.

Bachalo-Johnson Bump

This test case features the transonic interaction of a fully developed turbulent boundary layer with the pressure field created by a circular arc bump on the surface of a cylinder. The surface pressure distributions for various freestream Mach numbers are available, and velocity and Reynolds stress profiles are available for the $M_\infty = 0.875$ case.

Upstream boundary conditions were constant total pressure and temperature, with static pressure allowed to vary and velocity direction aligned with the cylinder axis. The outer edge of the flowfield was treated by extending the grid 8 bump chords away from the wall, and utilizing characteristic(no reflection) boundary conditions. The viscous wall(the surface of a cylinder) is a no-slip, adiabatic wall. The downstream static pressure was held at p_∞ Upstream length of the cylinder was adjusted to match computed boundary layer thickness at $x = -0.25m$ to experiment as done in the Driver case, and again this "entry length" was the same for all three models.

The grid for this case is 181(streamwise)×78(wall normal). Fine grid solutions with a 358 × 161 grid were indistinguishable to plotting accuracy, in terms of both surface pressures and velocity profiles at both $M_\infty = 0.875$ and $M_\infty = 0.925$ cases. The wall normal

grid spacing for both normal and fine grids had a y^+ less than 0.17 upstream of the shock.
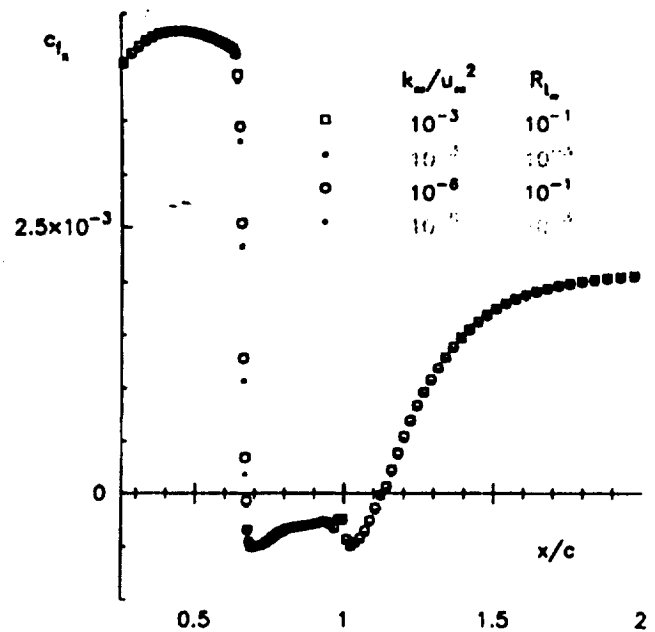

Fig. 10 $M\infty = 0.875$ Skin Friction Insensitivity to k_∞ and $R_{t\infty}$ values

The insensitivity of the solution to freestream choices of $R_{t\infty}$ and k_∞ is illustrated in Fig. 10. Here, the predicted x component of skin friction is shown for a range of choices of these parameters. The k_∞ range corresponds to an initial freestream turbulence intensities from 0.08% to 2.5%. The $R_{t\infty}$ range corresponds to initial eddy viscosities of from 0.1 to 10^{-3} molecular viscosity. The surface pressure prediction variations are just as insensitive to these variations in freestream turbulence values.

The Lag model reproduces the experimental pressure distributions (Fig. 11) as well as either the Spalart-Allmaras or Menter SST models, a distinct improvement over the underlying $k - \omega$ model, which consistently misses the shock location and underpredicts the extent of the flow separation.

The velocity profiles show the progression of the flowfield through the separation(Fig. 12). The Lag model predicts a separation point intermediate between the predictions of the SST and SA models, and has a flow recovery better than the SST, though it still does not recover as rapidly as experiment. In these velocity profiles, there is no obvious kink at the edge of the boundary layer in contrast to the CS0 flowfield.

The shear stress profiles(Fig. 13) show the Lag model's increased prediction of τ_{max} downstream of the separation point, though it is not as large as measured in the experiment. Note that this plot has the wall distance logarithmic, expanding the inner region of the boundary layer. There is a consistent underprediction of the stresses in the inner layer by all of the models in the separated region, and all the models
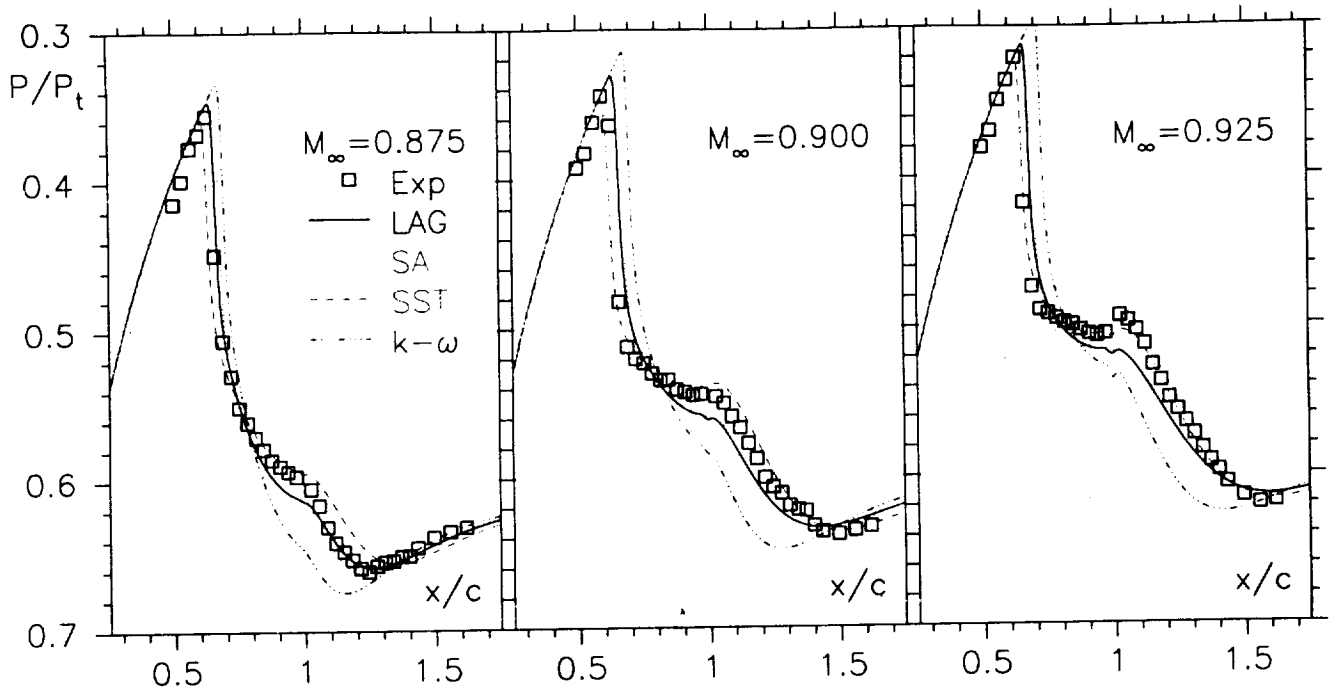
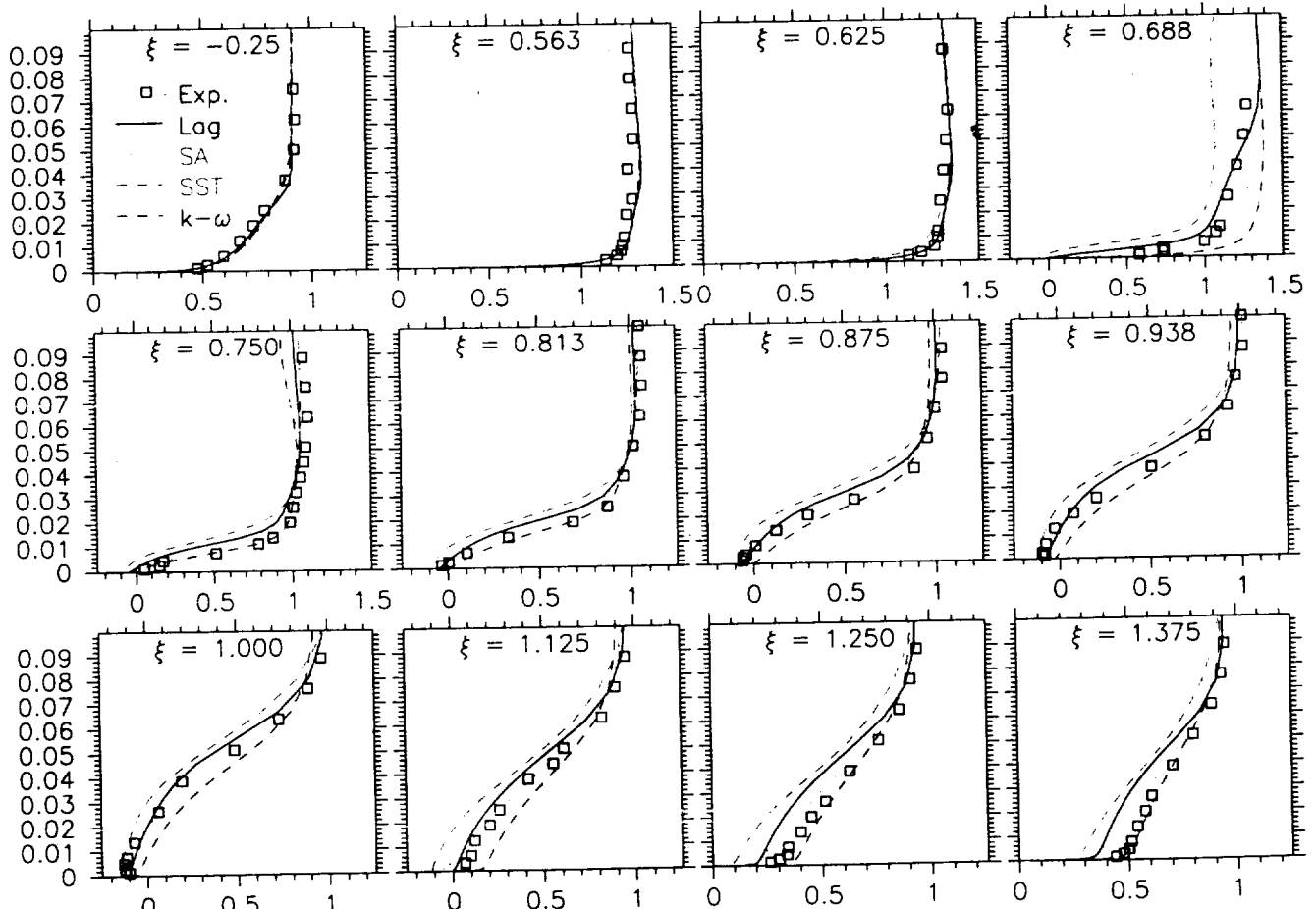**Fig. 11** Moo = 0.875, 0.900, 0.925 **Bachalo-Johnson Bump Pressure Distributions**

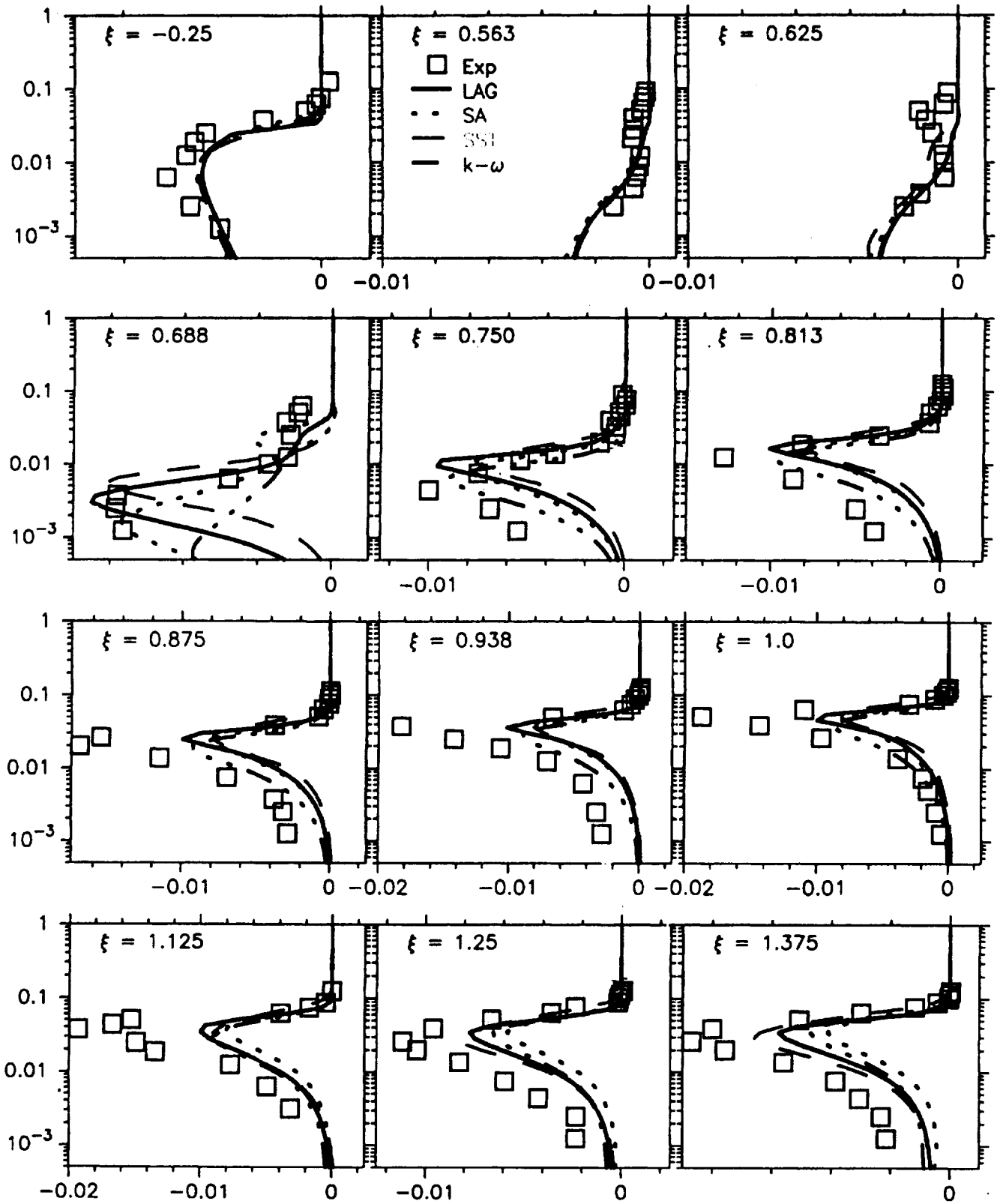**Fig. 12** **Bump Velocity Profile Comparisons, Moo = 0.875**

Fig. 13   Moo = 0.875 Bump Shear Stress Profiles

tween the predictions of the SST and SA models, and has a flow recovery better than the SST, though it still does not recover as rapidly as experiment. In these velocity profiles, there is no obvious kink at the edge of the boundary layer in contrast to the CS0 flowfield.

The shear stress profiles(Fig. 13) show the Lag model's increased prediction of τ_{max} downstream of the separation point, though it is not as large as measured in the experiment. Note that this plot has the wall distance logarithmic, expanding the inner region of the boundary layer. There is a consistent underprediction of the stresses in the inner layer by all of the models in the separated region, and all the models seriously underpredict the measured maximum shear stress.

ONERA M6 Wing

The ONERA M6[4] is a venerable 3D test case. In the conditions from $\alpha = 3°$ to $\alpha = 5°$ range from a nearly attached flowfield to a relatively extensive separation, as shown in Fig. 14.

The grid used in these computations was the one shipped as a test case with OVERFLOW, which has grid dimensions of 269(streamwise)×35(spanwise)×67(wall normal), with 201 points streamwise along the wing surface. The y^+ of the first point off the surface was below 1.25 over the entire wing surface. No grid resolution study was performed.

The C_p predictions of the model are compared with experiment in Fig. 15. The Lag model produces a good prediction over this entire range of conditions. The largest discrepancies in this range are at the wing root, and are more likely due to the tunnel wall interference, as the flow is attached in this region. As can be seen in the "oil flow" pictures of Fig. 14, all these cases have some separation, from a "incipient separation" at 3° to the rather extensively separated 5° case.

All four models give good predictions at $\alpha = 3°$ and $\alpha = 4°$ conditions, but at $\alpha = 5°$ the separation there is an appreciable difference in the predictions provided by the various models. The wing tip separation progression in particular appears to be well captured by both the Spalart-Almaras and the Lag model. The SST model has more extensive separation than experiment, and the separation predicted by the $k-\omega$ model is less extensive than experiment.

Discussion

The lag equation could be coupled to virtually any model. We have chosen to couple it to the $k-\omega$ model for this example. Another possible implementation would be to lag the Reynold's stresses, as opposed to the eddy viscosity, via an equation of the form

$$\frac{D\tau_{ij}}{Dt} = a'(R_T)\, \omega\, (2\mu_{t_\epsilon} s_{ij} - \tau_{ij})$$

to account for anisotropic effects seen in 3D flows.

The main feature of this new class of models is to introduce a lag into the response of the eddy viscosity to rapid changes in the mean flowfields so as to emulate the responses seen experimentally. Virtually all turbulence models generate Reynolds stresses that respond too rapidly to changes in mean flow conditions. Even the Reynolds stress models predict overly rapid response of the Reynolds stresses to changes in mean flow conditions. This is in large part due to the models' need to accurately reproduce equilibrium flows.

The lag equation gives the existing models an additional degree of freedom, without tampering with their typically good ability to predict equilibrium flows.

Summary

The Lag model gives good results for mild to moderate 2D separations, and agrees well with 3D cases tested. It works well for skin friction prediction at incompressible and supersonic Mach numbers, and predicts separation well for incompressible and transonic test cases. The model does not require wall distance, in contrast to both SST and SA models, and its simplicity is such that the computational effort is roughly equivalent to the simpler 1 and 2 equation models. Future work will include efforts to remove freestream effects, and will look at free shear flows, along with other experimental test cases.

References

[1]Wilcox, David C. . "Turbulence Modeling for CFD". DCW Industries, Inc, 1993.

[2]D.M. Driver. "Reynolds Shear Stress Measurements in a Separated Boundary Layer Flow ". AIAA Paper 91-1787, 1991.

[3]Bachalo, W.D. and D.A. Johnson. "Transonic Turbulent Boundary Layer Separation Generated on an Axisymmetric Flow Model". AIAA Journal, 24:437–443, 1986.

[4]Schmitt V. and Charpin F. "Pressure Distributions on the ONERA-M6 Wing at Transonic Mach Numbers". In AGARD Report, number 138 in AR, pages B1-1 – B1-44, 1979.

[5]Spalart, P.R. and S.R. Allmaras. "A one equation Turbulence Model for Aerodynamic Flows". La Recherche Aerospatiale, 1:5–21, 1994.

[6]Menter, F.R. "Two Equation Eddy Viscosity Model for Engineering Applications". AIAA Journal, 32:1299–1310, 1994.

[7]Bardina, Jorge E., Huang, Peter G., and Thomas J. Coakley. "Turbulence Modeling Validation, Testing, and Development". NASA TM 110446, April 1997.

[8]Buning, Pieter. G et al. Overflow user's manual. Version 1.8, NASA Ames Research Center, February 1998.

[9]Jespersen, D, Pulliam, T. H., and P.G. Buning. Recent enhancements to overflow. AIAA Paper 97-0664, January 1997.

[10]Swanson, R. C. and Eli Turkel. "On Central-Difference and Upwind Schemes". Journal of Computational Physics, 101:292–306, 1992.

[11]F.R. Menter. "Influence of Freestream Values on $k-\omega$ Turbulence Model Predictions". AIAA Journal, 30(6):1657–1659, 1992.

[12]Thomas J. Coakley. "Development of Turbulence Models for Aerodynamic Applications". AIAA Paper 97-2009, 1997.

[13]Hellsten, Antti and Seppo Laine. "Extension of the k-ω-SST Turbulence Model for Flows Over Rough Surfaces". AIAA Paper 97-3577-CP, AIAA AFM Conference, August 11-13 1997, New Orleans, LA, 1997.

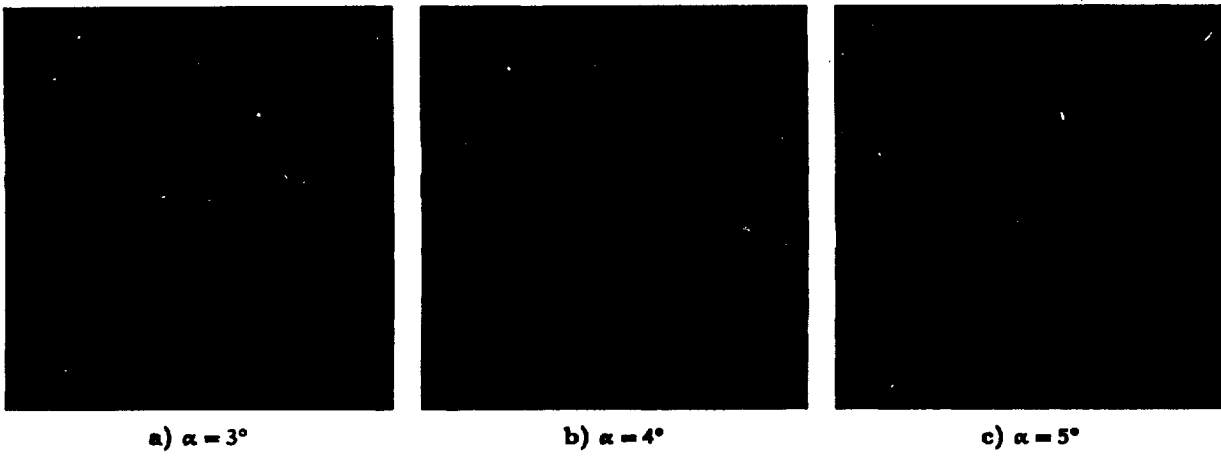a) $\alpha = 3°$　　b) $\alpha = 4°$　　c) $\alpha = 5°$

Fig. 14　Predicted Surface Flow(Lag Model), $M \approx 0.84$, $Re = 18 \times 10^6$
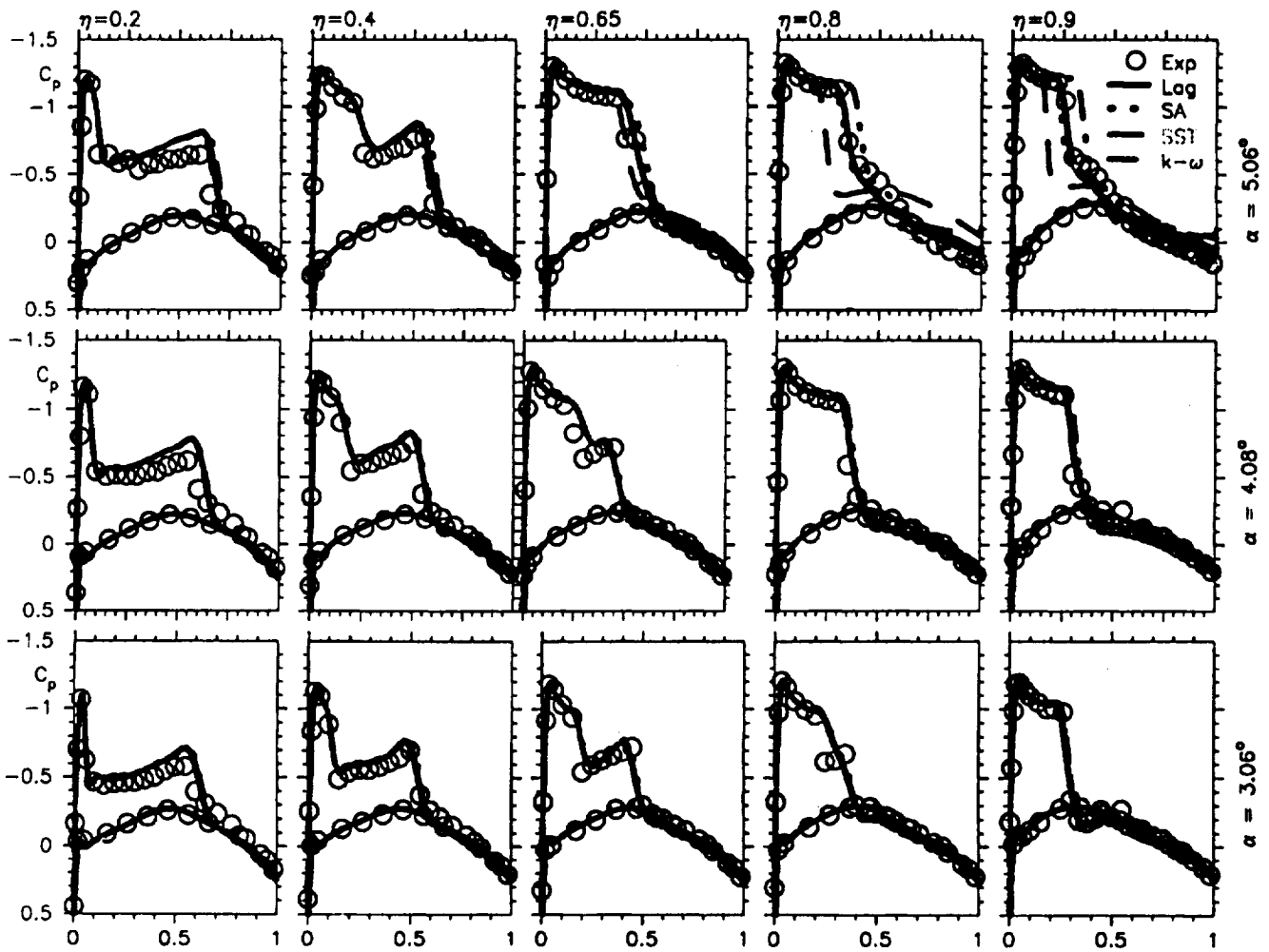

Fig. 15　ONERA M6 C_p Comparisons, $\alpha = 3, 4$ and $5°$

[14]Menter, Florian R. and Rumsey L. C. "Assessment of Two Equation Turbulence Models for Transonic Flows". AIAA Paper 94-2343, 1994.